Available online at www.sciencedirect.com
SCIENCE DIRECT
Journal of Power Sources 157 (2006) 488–493
JOURNAL OF POWER SOURCES
www.elsevier.com/locate/jpowsour

Morphological, structural, and electrochemical characteristics of $LiNi_{0.5}Mn_{0.4}M_{0.1}O_2$ (M = Li, Mg, Co, Al)

Decheng Li [a], Yuki Sasaki [b], Koichi Kobayakawa [b], Yuichi Sato [b,*]

[a] *High-Tech Research Center, Kanagawa University, 1-1-40 Suehiromachi, Tsurumi-ku, Yokohama 230-0045, Japan*
[b] *Department of Applied Chemistry, Faculty of Engineering, Kanagawa University, 3-27-1 Rokkakubashi, Kanagawa-ku, Yokohama 221-8686, Japan*

Received 12 May 2005; received in revised form 2 August 2005; accepted 2 August 2005
Available online 8 November 2005

Abstract

$LiNi_{0.5}Mn_{0.4}M_{0.1}O_2$ (M = Li, Mg, Al, Co) compound was prepared by a solid-state reaction, and its structural, morphological and electrochemical properties were characterized by XRD, SEM, charge–discharge tests and EIS. The impacts of alien ion introduction on the structural, morphological and electrochemical properties of $LiNi_{0.5}Mn_{0.5}O_2$ depend on the dopants. The substitution of Li, Mg, and Co for Mn can enlarge the particle size and improve the crystallinity. $LiNi_{0.5}Mn_{0.4}Li_{0.1}O_2$ and $LiNi_{0.5}Mn_{0.4}Co_{0.1}O_2$ show increased reversible capacities as well as upgraded rate capabilities. $LiNi_{0.5}Mn_{0.4}Li_{0.1}O_2$ exhibits a retentive capacity of about 200 mAh g^{-1} at 50 °C.

Keywords: Li-ion battery; Cathode material; $LiNi_{0.5}Mn_{0.4}M_{0.1}O_2$; Solid-state reaction; Electrochemical properties

1. Introduction

The Li–Ni–Mn–O system has been extensively investigated in this decade due to the potential application as cathode materials for lithium secondary batteries [1–5]. A layered $LiNi_{0.5}Mn_{0.5}O_2$, which was first reported by Spahr et al. [6], and re-proposed by Ohzuku and Makimura [7,8] and Dahn and co-workers [9,10], has been regarded as one of the most promising candidates. It has a highly reversible capacity (about 200 mAh g^{-1} in the voltage range of 2.5–4.5 V), good cyclic performance as well as excellent thermal stability. Nevertheless, it has some problems to be overcome in order to apply it in the future, such as the difficulty in the preparation [11], low tapping density [12] and poor rate capability [13]. The difficult preparation results from the prior formation of Li_2MnO_3 to the $LiNiO_2$ [14] and the electrochemically inert NiO is usually observed in the product prepared by the solid-state reaction. Therefore, $LiNi_{0.5}Mn_{0.5}O_2$ with a high electrochemical activity was usually synthesized through the solution process, such as the co-precipitation, a spray dry process and a sol–gel method. The low tapping density, which would reduce the energy density per volume, could be improved by means of the application of a sintering agent during the preparation [12,15]. The poor rate capability of $LiNi_{0.5}Mn_{0.5}O_2$, which means that the reversible capacity decreases significantly even the cell is operating at an intermediate current density, has been ascribed to its low electronic conductivity [13].

It is well known that foreign metal ion doping can upgrade the electrochemical properties of the cathode material. Generally, there are two kinds of substitution in terms of the charge balance. One is the equivalent and the other is the nonequivalent substitution. The equivalent-substituted $LiNi_{0.5}Mn_{0.5}O_2$, such as $LiNi_{0.5}Mn_{0.5-x}Ti_xO_2$ [11] and $LiNi_{0.50.5-x}Mn_{0.5-x}Co_{2x}O_2$ [16–20], has been extensively studied. However, investigation of the nonequivalent-substituted $LiNi_{0.5}Mn_{0.5}O_2$ is rather limited [21]. As a matter of fact, great improvement in the electronic conductivity was observed in $Li_{0.99}Nb_{0.01}FePO_4$ [22] and $LiCo_{1-x}Mg_xO_2$ [23] systems induced by the charge compensation.

In this study, the $LiNi_{0.5}Mn_{0.4}M_{0.1}O_2$ (M = Li, Mg, Al, Co) compound was prepared by a solid state reaction, and its structural, morphological and electrochemical properties were also provided.

* Corresponding author. Tel.: +81 45 481 5661x3885; fax: +81 45 413 9770.
E-mail address: satouy01@kanagawa-u.ac.jp (Y. Sato).

0378-7753/$ – see front matter © 2005 Elsevier B.V. All rights reserved.
doi:10.1016/j.jpowsour.2005.08.023

2. Experimental

Yoshio et al. [14] had reported that the Li_2MnO_3 formed at 400 °C while the $LiNiO_2$ formed at 680 °C, which is the main reason why $LiNi_{0.5}Mn_{0.5}O_2$ with a high purity is difficult to be prepared by the solid-state reaction. In order to avoid this problem and prepare samples with high electrochemical activities, we initially dispersed the stoichiometric starting materials, $Ni(OH)_2$ (Wako), $Mn(CH_3COO)_2{\cdot}4H_2O$ (Wako), $Mg(CH_3COO)_2{\cdot}4H_2O$ (Wako), $Al(OH)_3$ (Wako) and CoO (Wako), into acetone, and thoroughly mixed them. The obtained mixtures were first preheated at 450 °C for 6 h in N_2. After being ground, the resulting precursors were mixed with stoichiometric $LiOH{\cdot}H_2O$ (Kishida) and pressed into pellets. These pellets were sintered at 950 °C for 25 h in O_2 and then cooled to room temperature in the furnace.

The XRD measurements were carried out using a Rigaku Rint1000 diffractometer equipped with a monochromator and a Cu target tube.

The scanning electron microscope (SEM) study of the samples was performed using Hitachi S-4000 electron microscope.

The charge/discharge tests were carried out using a CR2032 coin-type cell, which consists of a cathode and lithium metal anode separated by a Celgard 2400 porous polypropylene film. The cathode contains a mixture of 20 mg of accurately weighed active materials and 13 mg of teflonized acetylene black (TAB-2) as the conducting binder. The mixture was pressed onto a stainless steel mesh and dried at 130 °C for 5 h. The cells were assembled in a glove box filled with dried argon gas. The electrolyte was 1 M $LiPF_6$ in ethylene carbonate/dimethyl carbonate (EC/DMC, 1:2 by volume).

The electrochemical impedance spectroscopy (EIS) was carried out using a home-made tri-electrode cell, using metallic lithium as the counter and reference electrodes and 1 M $LiPF_6$ in ethylene carbonate/dimethyl carbonate (EC/DMC, 1:2 in volume) as the electrolyte. Three miligrams of the active material was well mixed with 2 mg TAB-2 and pressed onto a stainless mesh with a geometrical area of about 0.75 cm^2.

3. Results and discussion

The SEM images of $LiNi_{0.5}Mn_{0.5}O_2$ and $LiNi_{0.5}Mn_{0.4}M_{0.1}O_2$ (M = Li, Mg, Co) are shown in Fig. 1. $LiNi_{0.5}Mn_{0.5}O_2$ has an agglomerated morphology and the size of the primary particle is in a nano-scale range. All of the substituted samples have the accumulation morphology, but the primary particles become well shaped and their size increases. These results suggest that foreign metal ion doping could improve the crystallinity of the $LiNi_{0.5}Mn_{0.4}M_{0.1}O_2$.

Fig. 2 shows the XRD profiles of $LiNi_{0.5}Mn_{0.5}O_2$ and $LiNi_{0.5}Mn_{0.4}M_{0.1}O_2$ (M = Li, Mg, Al, Co). All samples have layered features in terms of their XRD patterns, and all peaks can be indexed on the basis of α-$NaFeO_2$. However,

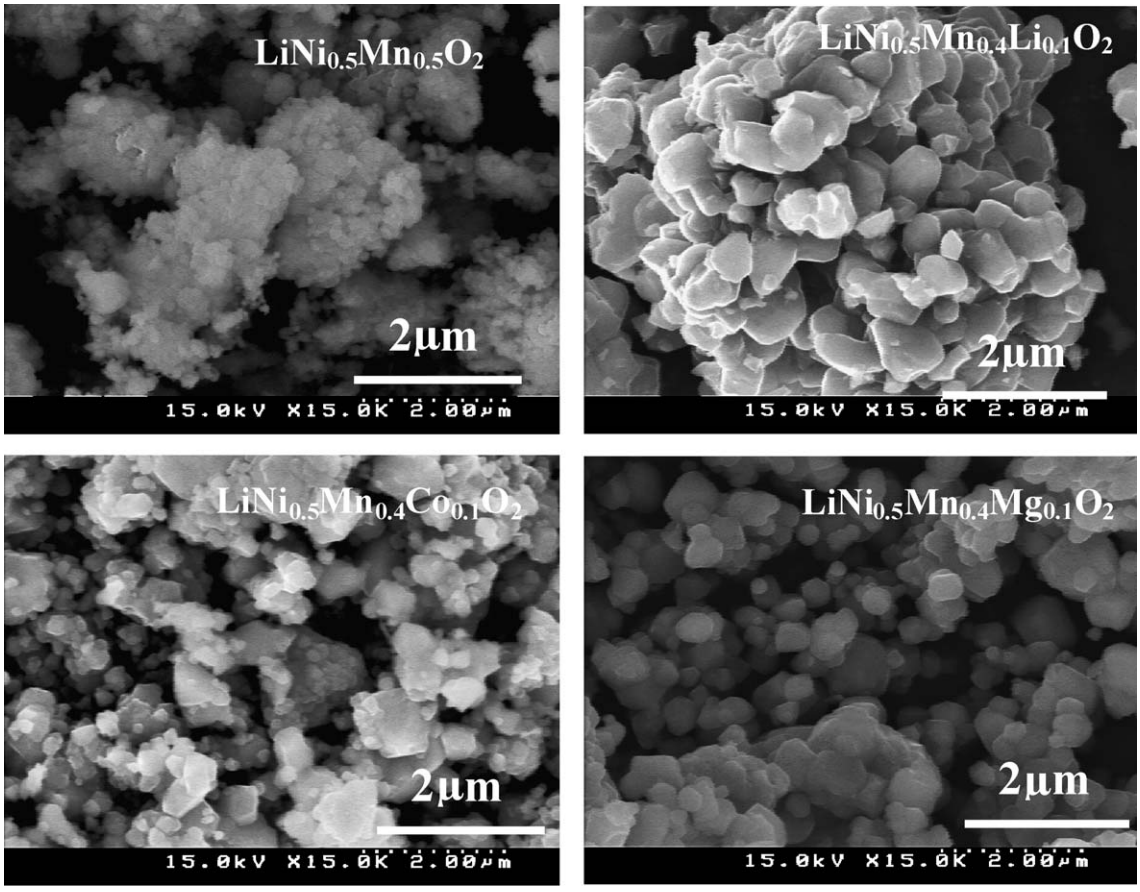

Fig. 1. SEM images of $LiNi_{0.5}Mn_{0.5}O_2$ and $LiNi_{0.5}Mn_{0.4}M_{0.1}O_2$ (M = Li, Mg, Co).

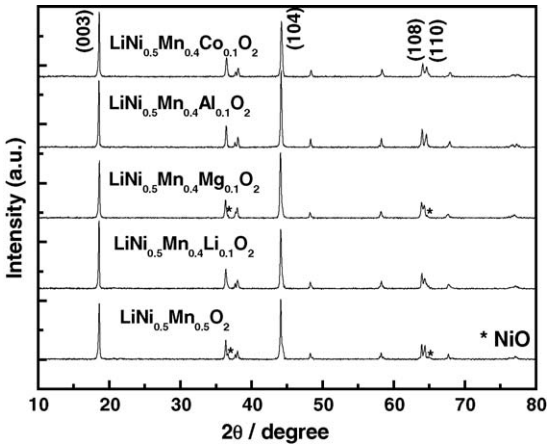

Fig. 2. XRD patterns of $LiNi_{0.5}Mn_{0.5}O_2$ and $LiNi_{0.5}Mn_{0.4}M_{0.1}O_2$ (M = Li, Mg, Al, Co).

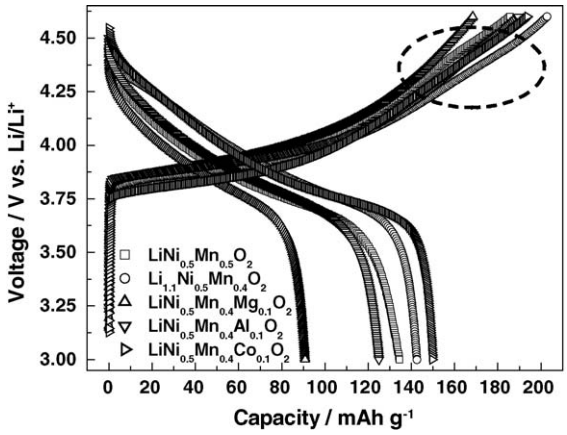

Fig. 3. Initial charge and discharge curves of $LiNi_{0.5}Mn_{0.5}O_2$ and $LiNi_{0.5}Mn_{0.4}M_{0.1}O_2$ (M = Li, Mg, Al, Co).

an impurity phase, NiO, appears in $LiNi_{0.5}Mn_{0.4}Mg_{0.1}O_2$ and $LiNi_{0.5}Mn_{0.5}O_2$. The diffraction peaks of the impurity phase cannot be observed in $LiNi_{0.5}Mn_{0.4}M_{0.1}O_2$ (M = Li, Al, Co), suggesting that the substitution of Li, Al, or Co can reduce the impurity content. Moreover, the doping of Co and Al causes clear splitting between (1 0 8) and (1 1 0), whereas these two peaks seem to merge into one peak in the cases of Li and Mg substitution. It is well known that the oxygen sub-lattice in the α-$NaFeO_2$ type structure forms a close-packed face centered cubic (*fcc*) lattice with a distortion in the *c* direction. Because of the slight distortion in the *c* direction, there are clearly splitting between (0 0 6/1 0 2) and (1 0 8/1 1 0) peaks in the XRD pattern. When this distortion in the *c* direction is absent (or the structure is totally cubic), the (0 0 6/1 0 2) and (1 0 8/1 1 0) peaks merge into single peaks in the diffraction pattern [24]. Our results suggest that Al and Co doping into $LiNi_{0.5}Mn_{0.5}O_2$ can increase the distortion in the *c* direction and the Al and Co doped samples have more layered features than the undoped one. In the case of Li and Mg substitution for Mn, the distortion in the *c* direction seems to be suppressed. We believed that this should be related to the large radius of Li^+ and Mg^+, because it is generally believed that the structure the compound adopts is primarily dependent on the of M in $LiMO_2$-type compounds and a compound with a small size of M can easily adopt the α-$NaFeO_2$ structure [25]. Thus, the substitution of Mg^{2+} with large ionic radius for Mn^{4+} increases the average ionic radius of M in $LiMO_2$ and makes the formation of the layered structure difficult.

The lattice parameters of $LiNi_{0.5}Mn_{0.5}O_2$ and $LiNi_{0.5}Mn_{0.4}M_{0.1}O_2$ (M = Li, Mg, Al, Co) were roughly calculated, and the results are summarized in Table 1. The lattice parameters of $LiNi_{0.5}Mn_{0.5}O_2$ are *a* = 2.891 Å, and *c* = 14.314 Å, well consistent with the reported results [7–10]. Generally, the impacts of dopants on the lattice parameters of $LiNi_{0.5}Mn_{0.4}M_{0.1}O_2$ are complex. Enlargement of the cell volume could be observed in the cases of $LiNi_{0.5}Mn_{0.4}Li_{0.1}O_2$ (or $Li_{1.1}Ni_{0.5}Mn_{0.4}O_2$) and $LiNi_{0.5}Mn_{0.4}Mg_{0.1}O_2$, which should be related to the larger radii of Li^+ (0.72 Å) and Mg^{2+} (0.78 Å) than that of Mn^{4+}(0.53 Å). $LiNi_{0.5}Mn_{0.4}Al_{0.1}O_2$ and $LiNi_{0.5}Mn_{0.4}Co_{0.1}O_2$ have shrunken cell volumes compared to that of $LiNi_{0.5}Mn_{0.5}O_2$. This seems to be abnormal because the size of Al^{3+} (0.57 Å) and Co^{3+} (0.545 Å) is bigger than that of Mn^{4+}, thus their cell volume should be expanded according to Vegard's law. We believe that this would be attributed to the decrease in the Ni^{2+} (0.69 Å) content caused by the charge compensation in order for the compound to remain in electrically neutral. On the other hand, the intensity ratios of I_{003}/I_{104} of $LiNi_{0.5}Mn_{0.4}Co_{0.1}O_2$ and $LiNi_{0.5}Mn_{0.4}Li_{0.1}O_2$ or $Li_{1.1}Ni_{0.5}Mn_{0.4}O_2$ (both are 1.14) increase significantly compared with that of $LiNi_{0.5}Mn_{0.5}O_2$ (0.92). It has been reported that if this value is <1.2 [26], the undesirable cation mixing would occur in the lattice. Our results suggest that Li and Co doping seems to alleviate the degree of cation mixing compared with the undoped one. The decrease in the *c*/*a* ratio of $LiNi_{0.5}Mn_{0.4}Mg_{0.1}O_2$ probably results from the severe cation mixing because it has the lowest intensity ratio of (0 0 3) to (1 0 4) peaks [27], as given in Table 1. It should be pointed that the chance in the intensity ratio of (0 0 3) peak to (1 0 4) peak depends not only on the degree of cation mixing, but also on the scattering factors of the dopants. Further works are necessary to quantitatively analyze the structural change caused by the alien metal substitution.

Table 1
The roughly calculated lattice parameters of $LiNi_{0.5}Mn_{0.4}M_{0.1}O_2$

Samples	*a* (Å)	*c* (Å)	*c*/*a*	*V* (Å^3)	I_{003}/I_{104}
$LiNi_{0.5}Mn_{0.5}O_2$	2.891	14.314	4.951	103.60	0.92
$LiNi_{0.5}Mn_{0.4}Li_{0.1}O_2$	2.893	14.330	4.954	103.83	1.14
$LiNi_{0.5}Mn_{0.4}Mg_{0.1}O_2$	2.896	14.299	4.948	103.84	0.87
$LiNi_{0.5}Mn_{0.4}Al_{0.1}O_2$	2.883	14.344	4.975	103.25	0.89
$LiNi_{0.5}Mn_{0.4}Co_{0.1}O_2$	2.883	14.290	4.967	102.86	1.14

The initial charge and discharge curves of $LiNi_{0.5}Mn_{0.5}O_2$ and $LiNi_{0.5}Mn_{0.4}M_{0.1}O_2$ (M = Li, Mg, Al, Co) are provided in Fig. 3. The cells were operated at a current density of 0.4 mA cm^{-2} in a 3–4.6 V range at room temperature. The initial charge and discharge capacities of $LiNi_{0.5}Mn_{0.5}O_2$ are 185 mAh g^{-1} and 135 mAh g^{-1}, respectively. All substituted samples except for $LiNi_{0.5}Mn_{0.4}Mg_{0.1}O_2$ exhibited lower cell polarization than that of $LiNi_{0.5}Mn_{0.5}O_2$. The enlargement of the cell polarization of $LiNi_{0.5}Mn_{0.4}Mg_{0.1}O_2$ is probably due to the presence of the impurity phase as well as the severe cation

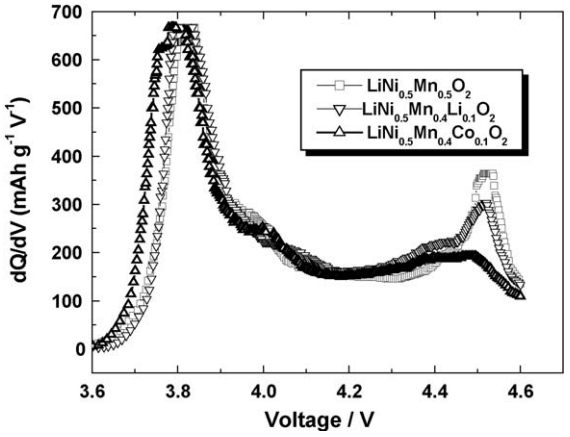

Fig. 4. dQ/dV curves of $LiNi_{0.5}Mn_{0.5}O_2$ and $LiNi_{0.5}Mn_{0.4}M_{0.1}O_2$ (M = Li, Co) at 50 °C.

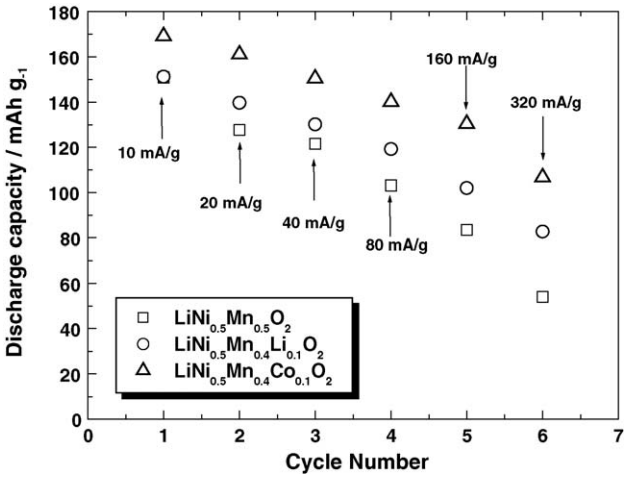

Fig. 5. Discharge capacities vs. discharge current densities of $LiNi_{0.5}Mn_{0.5}O_2$ and $LiNi_{0.5}Mn_{0.4}M_{0.1}O_2$ (M = Li, Co).

mixing. Moreover, $LiNi_{0.5}Mn_{0.4}Li_{0.1}O_2$ (or $Li_{1.1}Ni_{0.5}Mn_{0.4}O_2$) and $LiNi_{0.5}Mn_{0.4}Co_{0.1}O_2$ have increased charge and discharge capacities, while the discharge capacity of $LiNi_{0.5}Mn_{0.4}Al_{0.1}O_2$ decreased compared to that of $LiNi_{0.5}Mn_{0.5}O_2$. It is interesting to find that the shape of the initial charge curve changes after dopants are introduced into $LiNi_{0.5}Mn_{0.5}O_2$. A small plateau around 4.5 V can be observed in the initial charge curve of $LiNi_{0.5}Mn_{0.5}O_2$, and this plateau seems to disappear in the initial charge curves of those substituted samples. This difference can be clearly distinguished in their dQ/dV curves when the cells were operated at an elevated temperature.

Fig. 4 illustrates the dQ/dV curves of $LiNi_{0.5}Mn_{0.5}O_2$ and $LiNi_{0.5}Mn_{0.4}M_{0.1}O_2$ (M = Li, Co) at 50 °C. All curves contain two peaks. One is at about 3.8 V and the other is at about 4.5 V. The substitution of Li and Co for Mn reduced the capacity at the high voltage region (4.5 V). Noguchi and co-workers [14,28] had studied the influence of preparation methods on the electrochemical properties in the systems of $LiNi_{0.5}Mn_{0.5-x}Ti_xO_2$ and $LiNi_{1/3}Mn_{1/3}Co_{1/3}O_2$ and stated that samples prepared by a solid state reaction should be regarded as a solid solution rather than as compounds. Our results suggest that the compositional deviation to a solid solution, like $Li[Ni_xLi_{1/3-2x/3}Mn_{2/3-x/3}]O_2$, could be suppressed by Li or Co substitution. As a matter of fact, the capacity of the second plateau is part of the irreversible capacity in the initial cycle; therefore, $LiNi_{0.5}Mn_{0.4}Li_{0.1}O_2$ (or $Li_{1.1}Ni_{0.5}Mn_{0.4}O_2$) and $LiNi_{0.5}Mn_{0.4}Co_{0.1}O_2$ show a high reversible capacity compared with other samples. Moreover, the peak at the 3.8 V region shifts in a low voltage direction in the case of $LiNi_{0.5}Mn_{0.4}Co_{0.1}O_2$, implying that this sample probably has a good rate capability.

Fig. 5 shows the discharge capacities versus discharge current densities of $LiNi_{0.5}Mn_{0.5}O_2$ and $LiNi_{0.5}Mn_{0.4}M_{0.1}O_2$ (M = Li, Co). The cells were operated in the voltage range of 3–4.6 V at room temperature. The charge current density was kept at 10 mA g^{-1}, while the discharge current density changes from 10 mA g^{-1} to 20 mA g^{-1}, 40 mA g^{-1}, 80 mA g^{-1}, 160 mA g^{-1}, and 320 mA g^{-1} in the following cycles. As illustrated in Fig. 5, $LiNi_{0.5}Mn_{0.4}Li_{0.1}O_2$ and $LiNi_{0.5}Mn_{0.4}Co_{0.1}O_2$ have an improved rate capability compared to that of $LiNi_{0.5}Mn_{0.5}O_2$.

The discharge capacity at the discharge current density of 320 mA g^{-1} is about 110 mAh g^{-1} for $LiNi_{0.5}Mn_{0.4}Co_{0.1}O_2$, which is about 70% of its initial discharge capacity and better than that of $LiNi_{0.5}Mn_{0.5}O_2$ (only 55 mAh g^{-1}, about 35% of its initial discharge capacity).

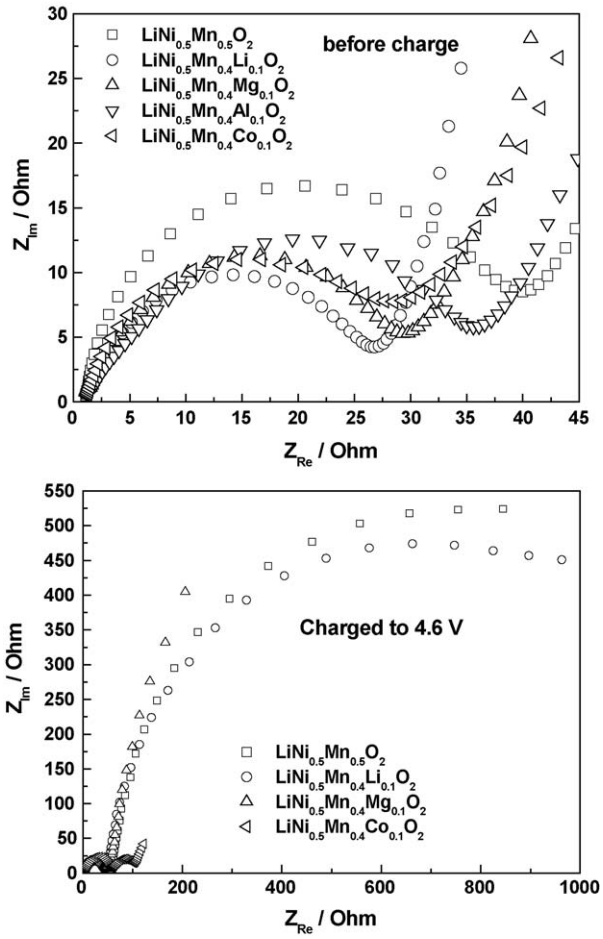

Fig. 6. Cole–Cole plots of $LiNi_{0.5}Mn_{0.5}O_2$ and $LiNi_{0.5}Mn_{0.4}M_{0.1}O_2$ (M = Li, Mg, Al, and Co) composite electrodes at different states-of-charge.

The Cole–Cole plots of $LiNi_{0.5}Mn_{0.5}O_2$ and $LiNi_{0.5}Mn_{0.4}M_{0.1}O_2$ (M = Li, Mg, Al, and Co) composite electrodes at different states-of-charge are illustrated in Fig. 6. One semicircle located in the high-frequency region was observed in these pristine composite electrodes in the frequency range from 20 kHz to 0.1 kHz, whose origin is probably related to the lithium ions migration through the interface between the surface layer of particles and the electrolyte, as addressed by Aurbach et al. [29,30]. $LiNi_{0.5}Mn_{0.4}M_{0.1}O_2$ (M = Li, Mg, Al, and Co) shows a decreased resistance compared with that of $LiNi_{0.5}Mn_{0.5}O_2$, suggesting that the metal ion substitution for Mn seems to improve the lithium ion migration through the surface layer. This semicircle seems to be unaffected if these electrodes were charged to 4.6 V. Moreover, a new semicircle appears in the low-frequency domain, whose origin could be ascribed to the charge-transfer resistance. $LiNi_{0.5}Mn_{0.4}Co_{0.1}O_2$ shows the smallest charge-transfer resistance, which probably results in the improved rate capability.

The cyclic performances of $LiNi_{0.5}Mn_{0.4}M_{0.1}O_2$ (M = Li, Mg, Al, Co) operating at room temperature and 50 °C are depicted in Fig. 7. The cells were operated at the current density of 0.4 mA cm^{-2} in the 3–4.6 V range. $LiNi_{0.5}Mn_{0.5}O_2$, $LiNi_{0.5}Mn_{0.4}Mg_{0.1}O_2$ and $LiNi_{0.5}Mn_{0.4}Al_{0.1}O_2$ showed poor reversible capacities at room temperature, while $LiNi_{0.5}Mn_{0.4}Li_{0.1}O_2$ and $LiNi_{0.5}Mn_{0.4}Co_{0.1}O_2$ had relatively high reversible capacities after 30 cycles. Their retention capacities are about 130 mAh g^{-1}. The reversible capacities for all samples increased when the cells were cycled at 50 °C. They also exhibited good cyclic performance with little capacity fading during cycling. $LiNi_{0.5}Mn_{0.4}Li_{0.1}O_2$ ($Li_{1.1}Ni_{0.5}Mn_{0.4}O_2$) has a reversible capacity of about 190 mAh g^{-1}.

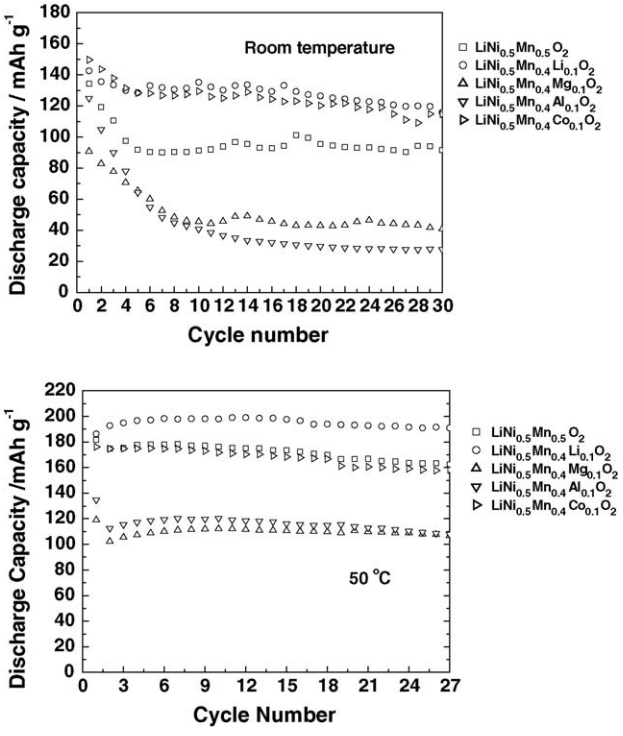

Fig. 7. Cyclic performances of $LiNi_{0.5}Mn_{0.5}O_2$ and $LiNi_{0.5}Mn_{0.4}M_{0.1}O_2$ (M = Li, Mg, Al, Co) operating at room temperature and 50 °C.

4. Conclusions

$LiNi_{0.5}Mn_{0.4}M_{0.1}O_2$ (M = Li, Mg, Al, Co) was prepared by a solid-state reaction. The nonequivalent substitution of metal ions for Mn in $LiNi_{0.5}Mn_{0.5}O_2$ could not only enlarge the size of the primary particles and improve the crystallinity, but also change the surface properties and promote the lithium ion migration in the surface layer. Upgraded rate capabilities were observed with $LiNi_{0.5}Mn_{0.4}Co_{0.1}O_2$, which should be attributed to the decrease in the charge-transfer resistance.

Acknowledgement

This work was financially supported by the High-Tech Research Center Project for Private University: matching fund subsidy from MEXT from 2001 to 2005.

References

[1] E. Rossen, C.D.W. Jones, J.R. Dahn, Solid State Ionics 57 (1992) 331.
[2] Y. Nitta, Y. Okamura, K. Harakuchi, S. Kobayashi, A. Ohta, J. Power Sources 54 (1995) 511.
[3] Q. Zhong, A. Bonakdarpour, M. Zhang, Y. Gao, J.R. Dahn, J. Electrochem. Soc. 144 (1997) 205.
[4] B.J. Neudecker, R.A. Zuhr, B.S. Kwak, J.B. Bates, J.D. Rebertson, J. Electrochem. Soc. 145 (1998) 4148.
[5] Y.S. Lee, Y.K. Sun, S. Ota, T. Miyashita, M. Yoshio, Electrochem. Commun. 4 (2002) 989.
[6] M.E. Spahr, P. Novak, B. Schnyder, O. Haas, R. Nesper, J. Power Sources 68 (1997) 629.
[7] T. Ohzuku, Y. Makimura, Chem. Lett. (2001) 744.
[8] Y. Makimura, T. Ohzuku, J. Power Sources 119–121 (1997) 156.
[9] Z. Lu, D.D. MacNeil, J.R. Dahn, Electrochem. Solid State Lett. 4 (2001) A191.
[10] Z. Lu, L.Y. Beaulieu, R.A. Donaberger, C.L. Thomas, J.R. Dahn, J. Electrochem. Soc. 149 (2002) A778.
[11] D. Li, T. Muta, H. Noguchi, J. Power Sources 135 (2004) 262.
[12] S. Jouanneau, J.R. Dahn, J. Electrochem. Soc. 151 (2004) A1749.
[13] B.L. Cushing, J.B. Goodenough, Solid State Sci. 4 (2002) 1487.
[14] M. Yoshio, Y. Todorov, K. Yamato, H. Noguchi, J. Itoh, M. Okada, T. Mouri, J. Power Sources 74 (1998) 46.
[15] S. Jouanneau, W. Bahmet, K.W. Eberman, L.J. Krause, J.R. Dahn, J. Electrochem. Soc. 151 (2004) A1789.
[16] D. Li, H. Noguchi, M. Yoshio, Electrochim. Acta 50 (2004) 425.
[17] Y. Sun, C. Ouyang, Z. Wang, X. Huang, L. Chen, J. Electrochem. Soc. 151 (2004) A504.
[18] Z. Lu, D.D. MacNeil, J.R. Dahn, Electrochem. Solid State Lett. 4 (2001) A200.
[19] D.D. MacNeil, Z. Lu, J.R. Dahn, J. Electrochem. Soc. 149 (2002) A1332.
[20] S. Jouanneau, D.D. MacNeil, Z. Lu, S.D. Beattie, G. Murphy, J.R. Dahn, J. Electrochem. Soc. 150 (2003) A1299.
[21] D. Li, Y. Sasaki, M. Kageyama, K. Kobayakawa, Y. Sato, J. Power Sources 148 (2005) 85.
[22] S.-Y. Chung, J.T. Bloking, Y.-M. Chiang, Nat. Mater. 1 (2002) 123.
[23] H. Tukamoto, A.R. West, J. Electrochem. Soc. 144 (1997) 3164.
[24] Y. Gao, M.V. Yakovleva, W.B. Ebner, Electrochem. Solid State Lett. 1 (1998) 117.
[25] R. Kanno, T. Shirane, Y. Inaba, Y. Kawamoto, J. Power Sources 68 (1997) 145.

[26] T. Ohzuku, A. Ueda, M. Nagayama, Y. Iwakoshi, H. Komori, Electrochim. Acta 38 (1993) 1159.
[27] J.N. Reimers, E. Rossen, C.D. Jones, J.R. Dahn, Solid State Ionics 61 (1993) 335.
[28] D. Li, T. Muta, L. Zhang, M. Yoshio, H. Noguchi, J. Power Sources 132 (2004) 150.
[29] D. Aurbach, M. Levi, E. Levi, H. Teller, B. Markovsky, G. Salitra, U. Heider, L. Heider, J. Electrochem. Soc. 145 (1998) 3024.
[30] M. Levi, G. Salitra, B. Markovsky, H. Teller, D. Aurbach, U. Heider, L. Heider, J. Electrochem. Soc. 146 (1999) 1279.